Face-offsetting polygon meshes with variable offset rates

Elissa Ross, Daniel Hambleton and Robert Aish

June 2, 2016

Abstract

Architectural designs are frequently represented digitally as plane-faced meshes, yet these can be challenging to translate into built structures. Offsetting operations may be used to give thickness to meshes, and are produced by offsetting the faces, edges or vertices of the mesh in an appropriately defined normal direction. In a previous paper, we described a face-offsetting algorithm for resolving the revised combinatorics of the offset mesh produced by face-offsetting (Ross and Hambleton 2015). That is, given an input mesh with no design constraints, the algorithm computes the *exact* offset by determining the new geometric and combinatorial structure of the offset mesh. One of the design freedoms available in that method is the opportunity to specify different offset distances on a per-face basis. In the present paper we consider the implications of this freedom.

One question of particular interest is: under what conditions does an offset mesh produced by variable rate face-offsetting also have a uniform distance edge-offset? To physically realise a mesh as a built structure usually requires that the mesh edges are used as the basis for structural members, with some structural depth. Therefore, given a mesh M it is particularly desirable to find an offset mesh M' in which the edges of M' are at a uniform perpendicular distance d from their corresponding edge in M. We present a description of meshes that admit uniform distance edge offsets as a consequence of a variable rate exact face offset, based on a graph-theoretic analysis of the underlying dual mesh. The potential advantage of this approach is that it can provide an opportunity to rationalise the physical realisation of the mesh as a constructible structure where all edge based members have the same depth.

keywords. offsetting polygon meshes, offset mesh, face offset, edge offset, graph theory, graph duality, algorithms, facade rationalization, architectural geometry, multi-layer construction

1 Introduction

Architectural geometry is a useful transitional system between the expressive intentions of the architect and the practical constraints involved in realising these intentions as a physically constructible building. Different types of geometry offer different design freedoms, but not all geometry is constructible, therefore it is also essential that geometric design tools are developed that present these freedoms and the limits to these freedoms. This is particularly important when dealing with doubly curved surfaces which are fundamentally at odds with most standardized manufacturing processes, such as sheet metal fabrication, extrusions, and glass panel manufacturing. While it is certainly possible to employ specialized construction techniques for such surfaces, there is considerable value in developing design technology that approximate continuously curving surfaces with collections of planar elements. This *discretization* process is of interest not just in architectural geometry, but also computer graphics, discrete differential geometry, physical simulations, and more.

In architecture, however, it is not enough to consider only the discretization of surface geometry. All physical objects have thickness, which is most often realized in the design phase by applying various *offsetting* techniques to the elements of the design. For surface geometry, and even planar discretizations of surface geometry, the offsetting operation is not fully understood. Of particular interest are face and edge offsetting techniques, which give layers or thickness to facial or edge elements respectively. Offsetting the vertices of a mesh is also possible, although it typically introduces a 'twist' in the structural support members connecting the original mesh with the offset mesh, which may present additional fabrication challenges (Aish, Verboon, and Fagerström 2014). Some significant approaches to the face- and edge-offsetting problem have focused on characterizing the mesh geometry that produces 'well-behaved' offset outcomes (Pottmann et al. 2007; Pottmann and Wallner 2008; Wang and Liu 2010). Recently, we presented a general algorithm for face-offsetting meshes which focused on analytically describing the offset node details for any geometry, without constraint on the input or output meshes, or any overlay of aesthetic criteria (Ross and Hambleton 2015). Each method appears to offer some advantages but may also present disadvantages.

In Section 2 we give a more detailed introduction to the face-offsetting algorithm presented in Ross and Hambleton 2015, and discuss the design considerations that arise in the context of face and edge offsetting. In the subsequent section, we provide several examples of one of the design freedoms of this method, specifically the ability to specify a different offset distance for each face member of the mesh. Section 4 will introduce the idea of a *face-edge offset mesh*: a mesh that admits a variable rate face offset such that edge-edge distances are uniform. In that section we prove our main result, namely the characterization of a class of face-edge offset meshes of particular interest in an architectural setting, using ideas from algebraic graph theory applied to the dual graph of the mesh. This is followed in Section 5 with a discussion about how face-edge offset meshes may be used in a design setting.

2 Exact Face Offsetting

A general algorithm for *exact face-offsetting* of polygon meshes was described in a previous paper by two of the authors (Ross and Hambleton 2015). Given any plane-faced polygon mesh M, and an offset distance $d \in \mathbb{R}$, the algorithm finds the new polygon mesh resulting from offsetting each face of M in its normal direction by distance d (if $d < 0$, the offset will be inward). Unlike other approaches to face offsetting (Pottmann et al. 2007; Pottmann and Wallner 2008; Wang and Liu 2010), which aim to find a *parallel mesh* M' that is combinatorially equivalent to M, our approach does not require that the combinatorics of the new mesh to match those of the original. In particular, the offset mesh will possess new mesh vertices and edges, although it will not possess new mesh faces (see Figure 1). This introduces a significant relaxation of the constraints on the offsetting problem, and allows us to treat all mesh combinatorics (triangular, quadrilateral, hexagon or mixed polygon), and all underlying mesh geometry (e.g. concave, convex, hyperbolic, etc.) using a single algorithm that permits both inward and outward offsetting. Several examples of the usage of this algorithm are provided in Section 3.

2.1 The perpendicular structure

One advantage of any method of face offsetting is that it produces a planar *perpendicular structure* joining the original mesh with the offset mesh (Figures 1 and 2). That is, given a mesh edge e connecting two faces F_i and F_j, the corresponding edge e' connecting the offset faces F_i' and F_j' will be parallel to e.[1] Joining the mesh edge e to the offset mesh edge e' at their respective end points therefore creates a planar quadrilateral, which we call a *principal member* of the perpendicular structure. New edges in the offset mesh that emerge as artifacts of our general method may be connected to their originating vertex to form a triangle, which we shall call *facelets*[2] (Figure 3). In this way, our offsetting method produces a perpendicular structure between the original mesh and its offset consisting only of planar quadrilateral principal members and triangular facelets. This is in contrast to other approaches to offsetting meshes which introduce a 'twist' and therefore a non-planarity in the perpendicular structure. In the work of Aish, Verboon, and Fagerström 2014, the edges of the offset mesh were used to create the primary support structure, while the edges of the original mesh were used to create a secondary 'carrier' frame for each of the glazing panels (based on the faces of the original mesh). However, connecting the primary structure to carrier frames required additional elements. This significantly added to the physical and visual complexity of the resulting

1. Provided that this offset edge e' exists. One of the main ideas in our previous paper (Ross and Hambleton 2015) is the notion of *global combinatorial change* under offsetting. Specifically, after a sufficiently large offset step, some edges may shrink to a vertex, and faces may split into two, or vanish completely. For the consideration of the perpendicular structure in the present paper, we assume no such global combinatorial change has occurred.

2. Thanks to Al Fisher for this name.

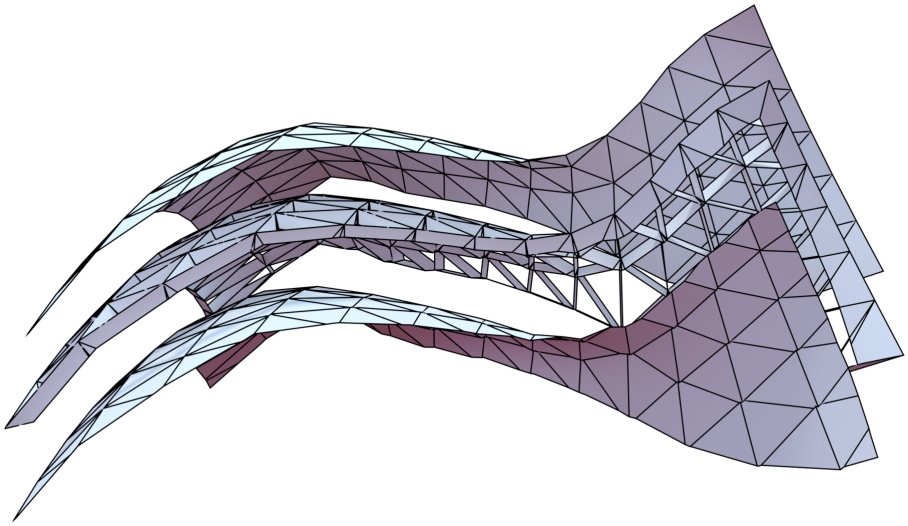

(a) The topmost mesh is the original design, and the bottom mesh is the face offset. Note that triangular mesh faces in the original have become polygonal mesh faces in the offset. The perpendicular structure can be seen in the middle layer, composed of planar quadrilateral *principal members* and triangular *facelets*.

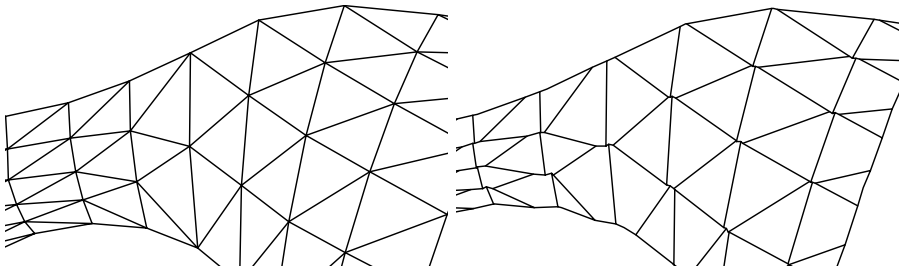

(b) original triangular mesh

(c) offset polygon mesh

Figure 1: A sample mesh offset with the exact face-offsetting algorithm.

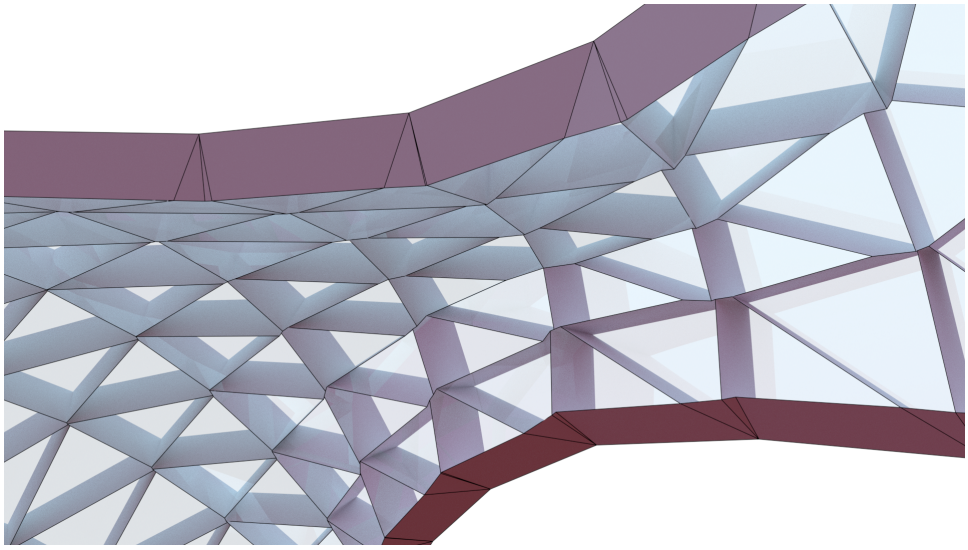

Figure 2: The perpendicular structure of the mesh shown in Figure 1.

architecture.

A question of interest in the context of the exact face offsetting algorithm is therefore: when do the principal members of the perpendicular structure have a uniform height? That is, when is it possible that a physical realization of the mesh as a constructible structure would have all edge-based members with the same cross-section? We answer this question in Section 4.

2.2 Design considerations in the perpendicular structure

While at first glance, the appearance of facelets may seem undesirable from a construction point of view, there is substantial design potential within this approach. For instance, it is certainly true that facelets which create crease angles or edge lengths that fall below manufacturing tolerances need to be eliminated from the design in order for the structure to be realized. However, by using the proposed polygonal mesh as basis, such conditions may be resolved using standard modelling operations such as filleting and chamfering (See Figure 4). Note that the planarity of the offset surface (which is guaranteed by our algorithm) becomes particularly important, since processing the planar offset faces is vastly simpler and more robust than processing more general surface geometry.

3 Offsetting with variable rates

One of the advantages of the face-offsetting method previously described (Ross and Hambleton 2015) is the ability to specify different offset distances on a

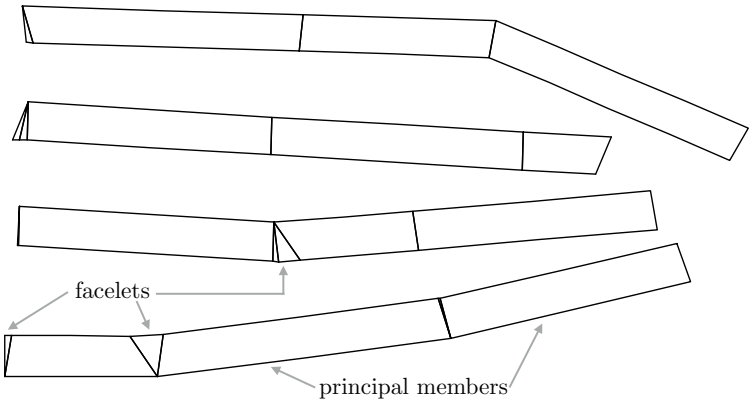

Figure 3: Unrolled perpendicular structure, with uniform edge offset height. Each row corresponds to a single face in an offset triangular mesh, and correspondingly has three principal members. The number of facelets depends on the offset geometry.

per-face basis. That is, rather than specifying a single offset distance $d \in \mathbb{R}$ to be applied to all faces of a mesh M, we may instead specify an offset vector $\vec{d} = (d_1, \ldots, d_{|F|})$ of distances, with one distance d_i for each face F_i. We call the vector of offset distances the *variable offset rates*.

A goal of this research is to explore how different 'design freedoms' or options might be offered to the architectural design team. In the remainder of this section we highlight the implications of the ability to specify different offset rates with several basic examples. Beyond these, one could also imagine offsetting a mesh surfaces with $\vec{d}$ determined parametrically, for example with a trigonometric function.

3.1 Example: offsetting a single face

In an extreme usage of variable rates, we set the offset rates of all faces to be zero, except one distinguished face which receives a positive offset rate. The result of the offset procedure is to completely "extrude" that distinguished face out of the mesh (Figure 5).

3.2 Example: fixing multiple faces

A second usage of variable rates might be to fix a section of a mesh, while offsetting the remainder (see Figure 6).

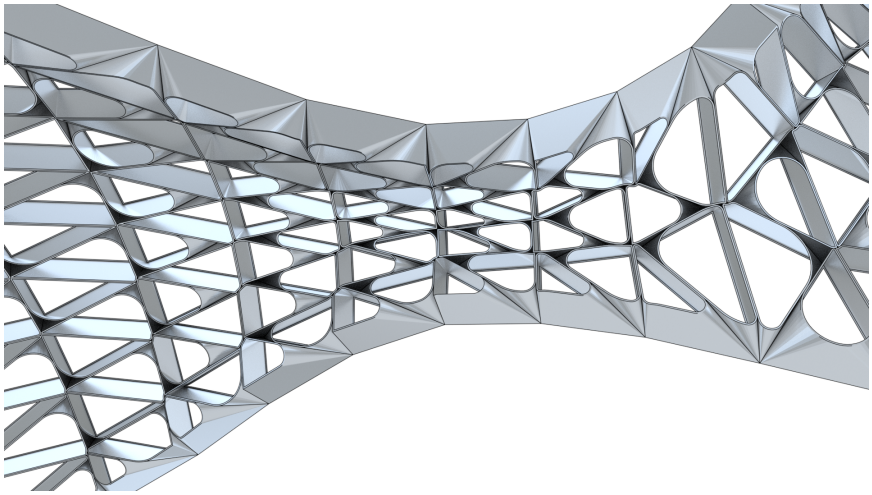

(a)

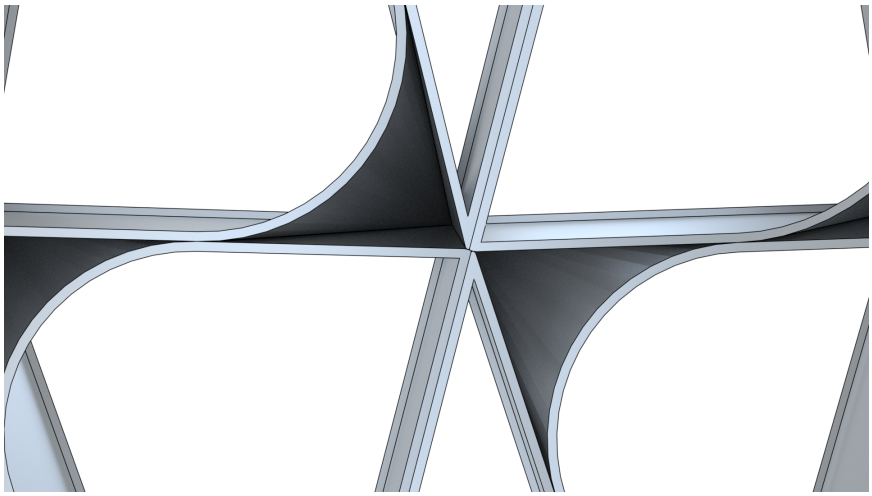

(b) detail

Figure 4: A filleting technique applied to the perpendicular structure.

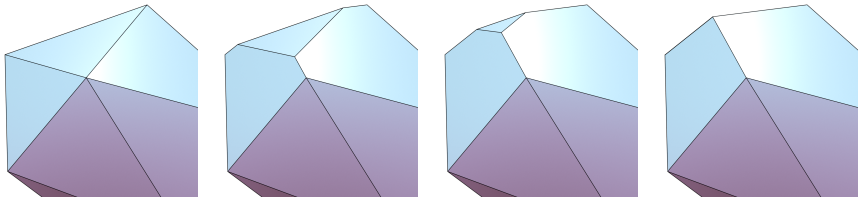

(a) original (b) (c) (d) final

Figure 5: Example of offsetting a single face only. The topmost face of the original mesh (a) will be extruded out of the mesh, leaving the final mesh (d) with one fewer face.

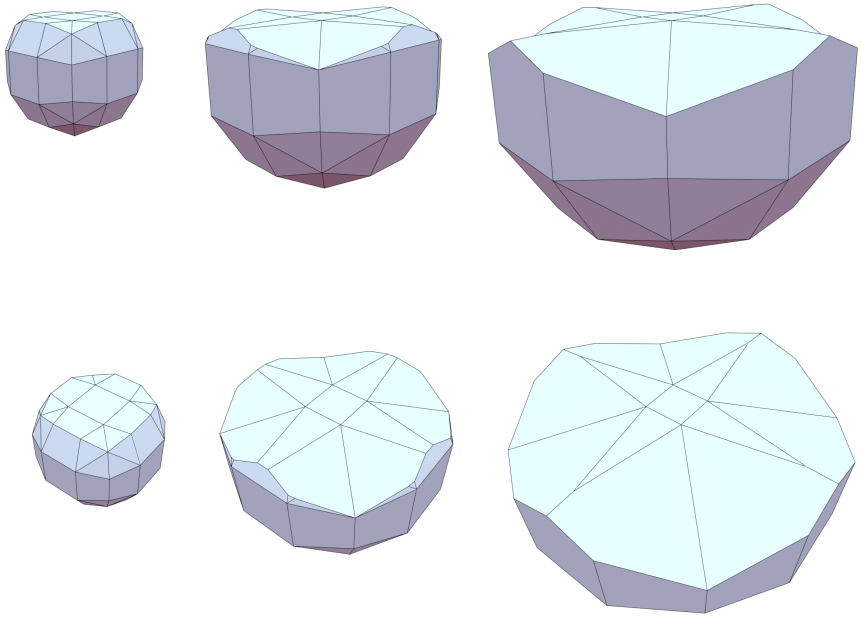

Figure 6: Example of offsetting with some fixed faces. Original mesh is shown at left, with the topmost faces fixed. Face-offsetting the other faces yields images at centre and right.

3.3 Example: rates determined by structural performance

In this final example, we consider a scenario in which it might be considered important that all faces be offset uniformly. The consequence of this "simplified" strategy is that some members will be over sized, therefore over weight, and therefore require an increase in the size of the other members. However, because all members should have the same cross-section, the whole structure may become less efficient and materially and visually heavy.

An alternative option might be to structurally optimise each member so as to reduce the face-face offset (and hence weight) of those members with less demanding role within the overall structure. Structural optimisation visually 'lightens' the architecture but may actually increases fabrication complexity. The approach of variable rate offsetting offers the architectural team both options. It does not constrain the architectural decision making, but rather defers to the team to make appropriate decision as to how to realise the mesh as a viable and efficient structure.

4 Edge offsetting as a consequence of face offsetting

In this section we outline a general theory for finding variable rate face offsets such that the resulting perpendicular structure has a uniform height on its principal members. More precisely, we say a mesh $M = (V, F)$ is a *face-edge-offset mesh*, or *FEO mesh* if there exists a set of rates $\vec{d} = (d_1, \ldots, d_{|F|}) \in \mathbb{R}^{|F|}$ such that face-offsetting M with rates $\vec{d}$ produces a mesh M' whose edges are at a uniform distance to the corresponding non-trivial edges of M. This will ensure that the principal members of the perpendicular structure have a uniform height. Note that this definition does not require that the facelets have uniform height from their originating vertex to the new edge.

4.1 A system of linear equations

Let $M = (V, E)$ be a mesh. Let e_{ij} be the edge connecting face F_i with F_j. Let α_{ij} be the interior angle between the faces. Viewed in the plane spanned by the normals of the faces, the planes F_i, F_j and their offsets generate a parallelogram (see Figure 7). The diagonal that divides the angle α_{ij} corresponds to the edge offset distance (shown in red), and here we normalize the edge offset distance to length $d = 1$. Let θ_i be the angle opposite the perpendicular distance d_i, which is the offset distance of face F_i.

Then for each interior mesh edge e_{ij} we have

$$\theta_i + \theta_j = \begin{cases} \alpha_{ij} & \text{if } 0 \leq \alpha_{ij} < \pi, \\ 2\pi - \alpha_{ij} & \text{if } \pi \leq \alpha_{ij} < 2\pi. \end{cases} \tag{1}$$

resulting in a system of linear equations.

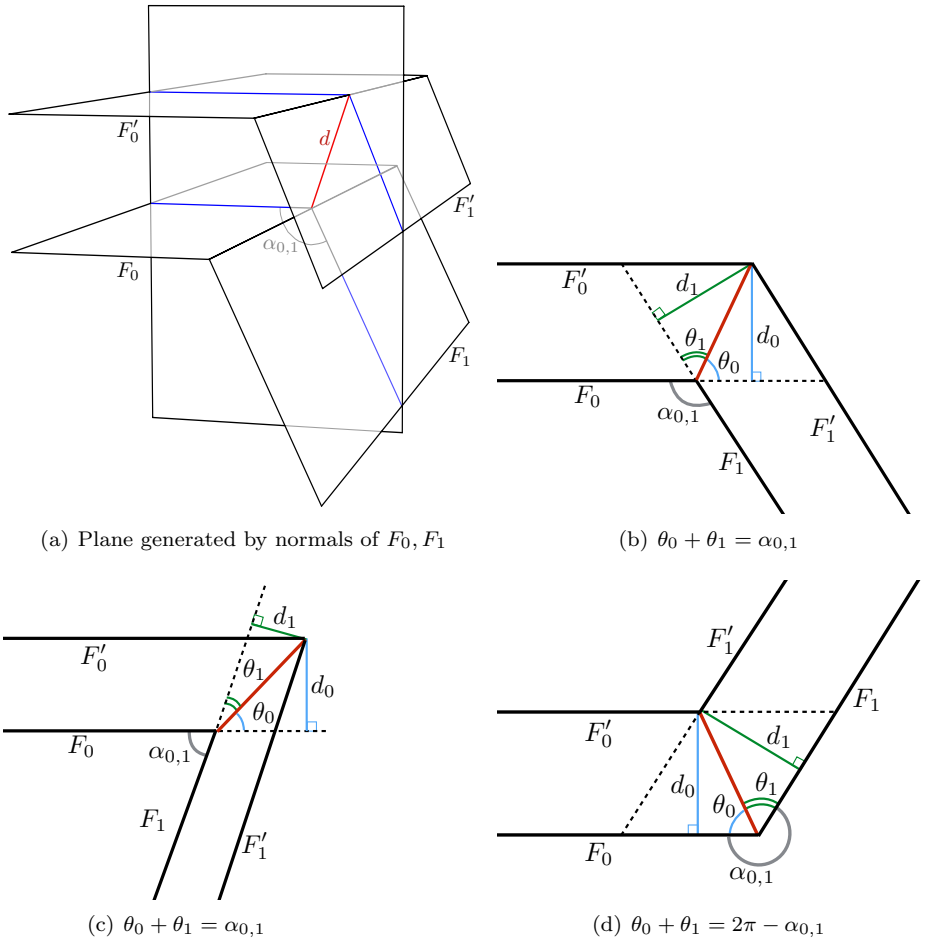

(a) Plane generated by normals of F_0, F_1

(b) $\theta_0 + \theta_1 = \alpha_{0,1}$

(c) $\theta_0 + \theta_1 = \alpha_{0,1}$

(d) $\theta_0 + \theta_1 = 2\pi - \alpha_{0,1}$

Figure 7: The plane P generated by the normals to faces F_0 and F_1 is shown in (a). The images in (b) – (d) are assumed to be in this plane P. The faces are lines in P, and the edge offset distance corresponds to the distance from the pairs of line intersections (shown in red). If the interior angle $\alpha_{0,1}$ between the faces F_0 and F_1 is less than π, then $\theta_0 + \theta_1 = \alpha_{0,1}$, otherwise $\theta_0 + \theta_1 = 2\pi - \alpha_{0,1}$.

If this system of equations has a solution, then we may recover the offset distances d_i by the formula $d_i = \sin(\theta_i)$. Note that for $\pi < \theta_i < 2\pi$, this value will be negative, indicating an inward offsetting plane.

Let

$$\beta_{ij} = \begin{cases} \alpha_{ij} & 0 \leq \alpha_{ij} < \pi, \\ 2\pi - \alpha_{ij} & \pi \leq \alpha_{ij} < 2\pi. \end{cases} \tag{2}$$

Then we may record the system of linear equations:

$$e_{ij} \begin{pmatrix} & & F_i & & F_j & & \\ & & \vdots & & & & \\ 0 \cdots 0 & 1 & 0 \cdots 0 & 1 & 0 \cdots 0 \\ & & \vdots & & & & \end{pmatrix} \begin{pmatrix} \theta_1 \\ \vdots \\ \theta_{|F|} \end{pmatrix} = \begin{pmatrix} \vdots \\ \beta_{ij} \\ \vdots \end{pmatrix}, \tag{3}$$

where $\vec{\theta} = (\ \theta_1 \quad \cdots \quad \theta_{|F|}\ )$ is a vector of length $|F|$, and $\vec{\beta} = (\ \cdots \quad \beta_{ij} \quad \cdots\ )$ is a vector of length corresponding to the number of interior edges of M. For convenience we denote by A the matrix of the linear system (3).

To summarize, a mesh M is a FEO mesh if and only if there exists $\vec{\theta} \in \mathbb{R}^{|F|}$ satisfying $A\vec{\theta} = \vec{\beta}$. If such a solution exists, we recover the vector $\vec{d}$ of offset rates on the mesh by $d_i = \sin(\theta_i)$, for each face $F_i \in F(M)$.

4.2 Graph theory notation

Several immediate observations about FEO meshes are available from the problem set up. We first introduce some notation and vocabulary from graph theory (See e.g. Diestel 2010 or West 2001). Let $M = (V(M), F(M))$ be a polygon mesh. The *dual graph* of M to be the graph $D_M = (V(D), E(D))$ formed from M by introducing a vertex v_i in $V(D)$ for every face of M. Two vertices v_i, v_j of D_M are connected by an edge if the corresponding faces F_i, F_j are both incident to the same edge. For an open mesh M, the edges $E(D)$ of the dual D will be in one-to-one correspondence with the interior (non-boundary) edges of M, and the vertices $V(D)$ will be in one-to-one correspondence with the faces of M. Two vertices of a graph are *adjacent* if they are connected by an edge. A *cycle* is a graph with an equal number of vertices and edges, whose vertices can be placed around a circle so that vertices appear consecutively around the circle if and only if they are adjacent.

4.3 Observations about FEO meshes

We observe:

1. The matrix A is the *incidence matrix* of the dual graph D_M of the mesh M. The rows of A are indexed by the interior edges of M, which correspond exactly to the edges $E(D)$ of the dual D_M. The columns of A are indexed by the faces of M, which correspond to the vertices $V(D)$ of the dual.

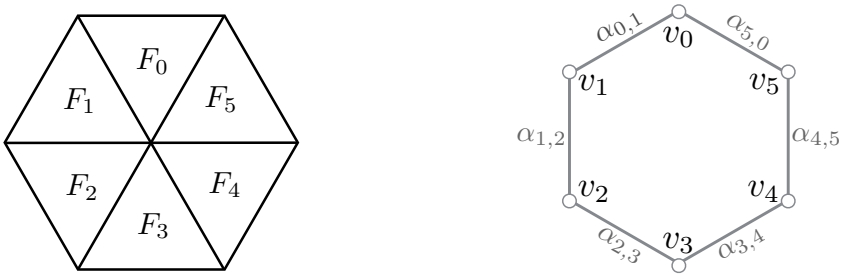

(a) M_6 (b) angle-labeled dual of M_6

Figure 8: A six-valent "fully-clothed" vertex mesh M_6 (a), and its hexagonal dual graph (b) with vertices corresponding to the faces of M_6, and edges labeled by the corresponding interior angles of M_6.

The incidence matrix of a graph $G = (V, E)$ is the $|E| \times |V|$ matrix $A(G)$ in which entry $A_{k,\ell}$ is 1 if vertex $v_\ell \in V$ is incident to edge $e_k \in E$, and 0 otherwise. Hence we may study the properties of M via the incidence matrix of its dual.

2. Each interior edge e of the mesh M corresponds to an entry of $\vec{\beta}$ containing the interior angle of the faces meeting at e. Because each interior edge of the mesh corresponds with an edge of the dual, the interior angles of the mesh M can be viewed as labels or weights on the (undirected) edges of D_M. In this way, the combinatorial and geometric information we require from M is stored in its edge-labeled dual graph D_M. See Figure 8 for a simple example. A solution to (3) can be interpreted as an assignment of an angle θ_i to each vertex v_i of the dual graph.

3. Unless the dual graph is a *tree* (a connected graph containing no cycles) or a connected *map-graph* (a connected graph containing exactly one cycle), the matrix A will have more rows than columns, and (3) is therefore an over-constrained system of equations. In other words, no solution to the linear system should be expected to exist in general. We shall see in the Section 4.5 exactly when a solution does exist.

4. Even if a solution to (3) does exist, it need not be a positive solution. That is, it may contain a combination of positive and negative offset rates (i.e. faces moving both inside and outside the mesh), which we assume to be undesirable in an architectural context. A question of interest is to determine under what conditions we can guarantee a solution with all positive rates.

4.4 Small examples

The meshes consisting of a single "fully-clothed" vertices form an interesting class of examples. Consider a mesh M_5 with one central vertex, and five incident faces. Similarly, let M_6 be the mesh consisting of one central vertex and six incident faces (see Figure 8(a)). The dual graphs corresponding to these meshes are a pentagon and hexagon respectively (8(b)). The augmented matrices for the linear system (3) are:

$$\left[\begin{array}{ccccc|c} 1 & 1 & 0 & 0 & 0 & \beta_{0,1} \\ 0 & 1 & 1 & 0 & 0 & \beta_{1,2} \\ 0 & 0 & 1 & 1 & 0 & \beta_{2,3} \\ 0 & 0 & 0 & 1 & 1 & \beta_{3,4} \\ 1 & 0 & 0 & 0 & 1 & \beta_{4,0} \end{array}\right] \quad \text{and} \quad \left[\begin{array}{cccccc|c} 1 & 1 & 0 & 0 & 0 & 0 & \beta_{0,1} \\ 0 & 1 & 1 & 0 & 0 & 0 & \beta_{1,2} \\ 0 & 0 & 1 & 1 & 0 & 0 & \beta_{2,3} \\ 0 & 0 & 0 & 1 & 1 & 0 & \beta_{3,4} \\ 0 & 0 & 0 & 0 & 1 & 1 & \beta_{4,5} \\ 1 & 0 & 0 & 0 & 0 & 1 & \beta_{5,0} \end{array}\right].$$

Row reduction to row-reduced echelon form already hints at some subtlety present in the problem. The incidence matrix A_5 of the 5-cycle row-reduces to the identity matrix I_5, which yields an exact solution to the system (3). In other words, for any combination of interior angles, a set of rates determining an edge offset always exists, and hence M_5 is always an FEO mesh.

On the other hand, row reduction of the matrix A_6 produces a dependent row. Therefore, for a solution to (3) to exist, we have additional conditions on $\vec{\beta}$ to ensure that it is in the column space of A_6. The row operations on the vector $\vec{\beta}$ yield the following condition on the adjusted interior angles:

$$\beta_{0,1} - \beta_{1,2} + \beta_{2,3} - \beta_{3,4} + \beta_{4,5} - \beta_{5,0} = 0.$$

In fact, this is true more generally for a vertex mesh M_n with a single central vertex of valence n: if n is odd, M_n will always be an FEO mesh. If n is even, then M_n will be an FEO mesh if and only if it satisfies the *alternating angle condition*:

$$\sum_{k=0}^{n-1} (-1)^k \beta_k = 0, \tag{4}$$

where β_k are the adjusted interior angles defined in (2) taken in cyclic order around the central vertex of M_n.[3]

4.5 Main result

The examples of the previous section highlight the fact that the properties of the underlying dual graph of the mesh play a role in determining the solution to the system (3). Before stating our main result, we first add to our vocabulary of graph theory terminology. A graph $G = (V, E)$ is *bipartite* if its vertices

3. When $n = 4$, this is equivalent to the condition found for conical mesh vertices in Wang, Wallner, and Liu 2007. For $n > 4$, a mesh vertex is not guaranteed to be conical even when it satisfies the alternating angle condition.

can be partitioned into two sets, such that a vertex in one set is connected only to vertices of the other set. We can think of this as a colouring of the vertices of the graph into two colours, so that no two adjacent vertices have the same colour. It is not hard to see that no odd cycle (e.g. a triangle) is bipartite, but every even cycle is bipartite. In fact, the absence of odd cycles characterizes bipartite graphs. Examples of meshes with bipartite duals are the planar quadrilateral meshes, and triangle meshes in which all vertices have even degree. It is straightforward to check whether a given graph is bipartite using a breadth-first search. We say a mesh is *simply-connected* if it does not have any holes.

Theorem 4.1. *Let M be a simply-connected mesh with a bipartite dual graph D_M. Then M is an FEO mesh if and only if the alternating angle condition is satisfied at every interior vertex of M.*

Before we prove this result, we require a few additional ideas from algebraic graph theory, which are adapted from the work of Grossman, Kulkarni, and Schochetman 1994. Let $G = (V, E)$ be a graph. A *circulation* f on E is a real-valued function on the edge set of G such that, for each vertex v, the sum of $f(e)$ taken over all edges incident to v is zero. In particular, we may define the *circulation f_C induced by a cycle* $C = \{e_{j_0}, e_{j_1}, \ldots, e_{j_r}\}$ to be

$$f(e) = \begin{cases} 0 & e \notin C, \\ 1 & \text{if } e \text{ appears in } C \text{ as } e_{j_k},\ k \text{ odd}, \\ -1 & \text{if } e \text{ appears in } C \text{ as } e_{j_k},\ k \text{ even}. \end{cases}$$

It is not hard to show that the set of all circulations on a graph is a vector space, and we call this the *circulant space*, denoted by $\mathcal{C}_0$. We summarize some useful facts about this vector space in the following statement, although it should be noted that the original statements in Grossman, Kulkarni, and Schochetman 1994 are far more general (see also Remark 4.3 in this paper).

Theorem 4.2 ((Grossman, Kulkarni, and Schochetman 1994), Theorems 4.1 and 5.5)**.** *For a graph G, the circulant space $\mathcal{C}_0$ is equal to the nullspace of the transpose of the incidence matrix of G. If G is bipartite, then a basis for $\mathcal{C}_0$ is induced by a basis of the cycle space of G (which, because G is bipartite, consists exclusively of even cycles).*

We are now able to prove our main result.

Proof of Theorem 4.1. Let M be a mesh with bipartite dual D_M. If M is an FEO mesh, then a solution $\vec{\theta}$ exists for the linear system $A\vec{\theta} = \vec{\beta}$ (3) where A is the incidence matrix of D_M and $\vec{\beta}$ is the vector of adjusted interior angles of the mesh M. Then $\vec{\beta}$ is in the column space of A. The column space of A is the orthogonal complement of the null space of A^T (see e.g. Strang 2009). Therefore $\vec{\beta}$ is orthogonal to every basis vector of $\ker(A^T)$. By Theorem 4.2, $\ker(A^T)$ is the circulant space $\mathcal{C}_0$ of D_M, which has a basis induced by the even

cycle space of D_M. Because D_M is bipartite, the even cycle space is equivalent to the cycle space of D_M. Because D_M is the dual of a simply-connected mesh, it is planar. Therefore, a basis for the cycle space of D_M is provided by the facial cycles around vertices (see e.g. Diestel 2010, 101). The circulation induced by a facial cycle is equivalent to the alternating angle condition at that interior vertex. The vector $\vec{\beta}$ of interior angles is orthogonal to a basis vector of $\mathcal{C}_0$ if and only if the alternating angle condition is satisfied at every interior vertex. The argument reverse for the converse. □

Remark 4.3. Extensions for the non-bipartite case, and the case of meshes that are not simply connected are easily available using the results of Grossman, Kulkarni, and Schochetman 1994: In the case of a mesh with dual graph that is not bipartite, a basis for the circulant space $\mathcal{C}_0$ is generated by the even cycles and *bow-ties*, which consist of two odd cycles joined by a path. In the case of a mesh that is not simply connected (i.e. it has holes), the circulant space can no longer be said to be generated by the facial cycles around vertices, but there is an equivalent condition on the even cycles and bow-ties. In these broader settings Theorem 4.1 can be adapted to characterize FEO meshes using the same basic proof. In all cases, the characterization of FEO meshes depends on an analysis of the even cycle space. Furthermore, the even cycle space of a graph G can be identified using a greedy algorithm, due to the underlying matroidal structure of this space (Grossman, Kulkarni, and Schochetman 1994, 295–296). □

It is known that the rank of the incidence matrix of a connected bipartite graph is $(|V| - 1)$ (Grossman, Kulkarni, and Schochetman 1994). That is, the columns of the incidence matrix of a bipartite graph are always dependent. This implies that, for meshes with a bipartite dual, the system of equations (3) has either no solutions or it has a one-parameter family of solutions. Provided a solution does exist, the following lemma provides us with a method for traversing the solution space of (3).

Lemma 4.4. *Let M be a simply-connected mesh, with bipartite dual graph D_M. Suppose $\vec{\theta}$ is a solution to (3), and let $\gamma \in [0, 2\pi)$. Let $\vec{\theta'}$ be the vector generated from $\vec{\theta}$ by adding γ to the entries corresponding to the vertices $v \in V(D)$ of one partition and subtracting γ to the entries corresponding to the vertices of the other partition. Then $\vec{\theta'}$ is also a solution to (3).*

Proof. The row of the matrix A of (3) corresponding to the edge $e_{i,j} = (v_i, v_j)$ is:

$$\theta_i + \theta_j = \alpha_{ij}.$$

Since v_i and v_j are adjacent vertices in D_M, they must be in different partitions. Then

$$(\theta_i + \gamma) + (\theta_j - \gamma) = \alpha_{ij}.$$

□

From a design perspective, we wish to find the "best" set of rates in this solution space. In most cases, this will be the set of rates that will minimize the

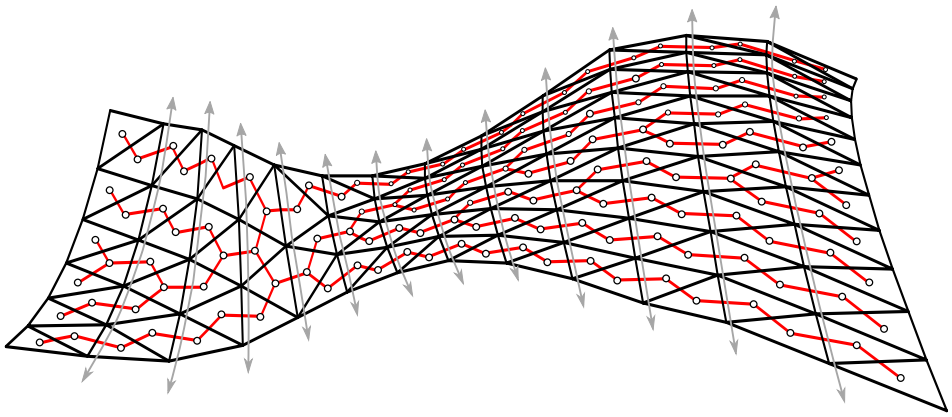

Figure 9: Schematic representation of the original mesh in Figure 1. The red edges form a spanning tree in the dual graph. Note that the red edges cross over every 'vertical' line of the mesh, indicated by the arrows. In this way, we can guarantee that the principal members of the perpendicular structure on these 'vertical beams' have a uniform height.

deviation among the offset distances for the faces of the mesh. If two adjacent faces F_i, F_j are offset to the same distance, then $\theta_i = \theta_j = \alpha_{ij}/2$. Therefore, to find the set of face offset rates which most closely emulate this, we find γ such that the adjusted angle vector θ' minimizes the sum

$$\sum_{\alpha} |\alpha_{ij}/2 - \theta'_i|.$$

5 Designing with variable rate face offsetting

In this section we consider several additional ways of designing using variable rate face offsetting beyond those outlined in Section 3. In particular, we consider two ways of working with FEO meshes, one which works on any mesh, and one which involves moving an original design toward an optimal solution.

5.1 Specifying a spanning tree of uniform edge offsets

For any mesh with $|F(M)|$ faces, we can always ensure that $|F(M)| - 1$ edges of the mesh have a uniform edge offset. In particular, we are free to chose a spanning tree (or spanning forest) in the dual mesh that captures the edges of interest (Figure 9). A *spanning tree* is a subgraph $T \subset D_M$ that contains no cycles and satisfies $V(T) = V(D_M)$. We then record only the edges of interest in (3), and solve to find the appropriate offset rates. In this way we could specify lines of 'beams' to offset with uniform edge distance, as indicated in Figure 9.

5.2 Evolving the mesh toward an FEO mesh

A second way to design with FEO meshes is to evolve an original design toward an FEO mesh. This work is still in a preliminary state, but our initial explorations indicate that the alternating angle condition is quite forgiving, and a wide range of geometries satisfying this condition are possible.

To illustrate the general idea, consider a small example mesh $M = M_6$, a single "fully-clothed" vertex v_0 with six incident faces, as in Section 4.4. The dual graph is bipartite, consisting of a single hexagon cycle, and therefore by Theorem 4.1 this is an FEO mesh if and only if the alternating angle condition is satisfied on the facial cycle corresponding to the single interior vertex v_0 of M.

To find the closest FEO mesh, we fix the positions of the neighbouring vertices, and use gradient descent on the position of v_0 to evolve the mesh M toward a new mesh M' satisfying the alternating angle condition. The resulting mesh is overlaid on the original mesh in Figure 10(a). Note that this movement is "small" in the sense that the basic geometric shape (which is hyperbolic) of the underlying mesh at that vertex is preserved.

The solution $\vec{\theta}$ to the linear system corresponding to M' is a one-parameter family, and using Lemma 4.4 we add a correction vector to the solution to find a new solution $\vec{\theta'}$ of angles such that $0 \leq \theta'_i < \pi$. We recover the offset rates by taking the sine of the vector $\vec{\theta'}$, and finally offset the mesh using these rates[4]. The perpendicular structures of the original mesh and the evolved versions are shown in Figure 10(b) and 10(c).

In a more complex example such as an architectural shell, the neighbouring vertices would not be fixed, but rather would be moving according to their own angle optimizations. In this sense, the optimization becomes highly nonlinear. It is possible to use the gradient descent method mentioned above on any input mesh. However, the result may not satisfy the same design criteria as the original. Therefore, a more holistic approach to the optimization would incorporate other constraints, for example, edge length, approximate position, equal area mesh faces, planarity for non-triangular faces, etc. The development of a full-featured optimization tool with design-based constraints is a topic for further research.

6 Conclusion and further work

Exact face offsetting with variable rates is a tool which offers a wide range of design possibilities, as illustrated through the examples in Section 3. Through the additional theory of FEO meshes, Section 5 offers several more techniques for ensuring that a mesh is not only a face offset, but is also a uniform edge offset on its principal members.

The work on FEO meshes remains in a preliminary state, and there are several questions of interest to address. Specifically, under what conditions can

4. $\vec{d} = (0.883, 0.753, 0.896, 0.905, 0.925, 0.987)$

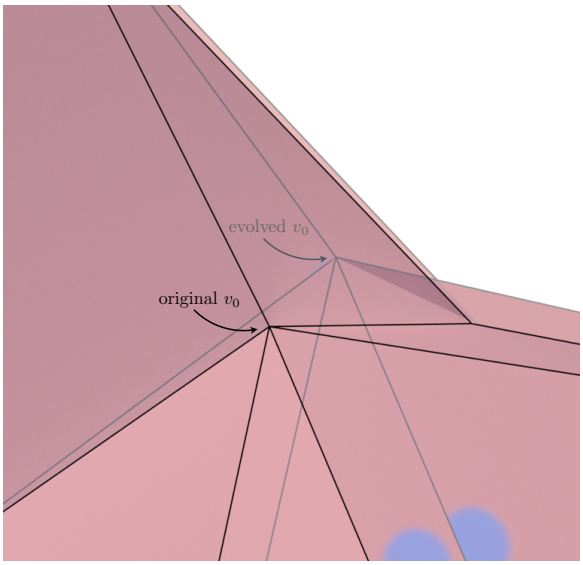

(a) Overlapped meshes. The facial cycle around the evolved vertex v_0 satisfies the alternating angle condition.

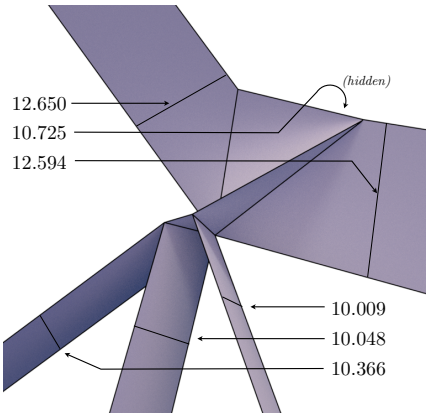

(b) Perpendicular structure, original mesh

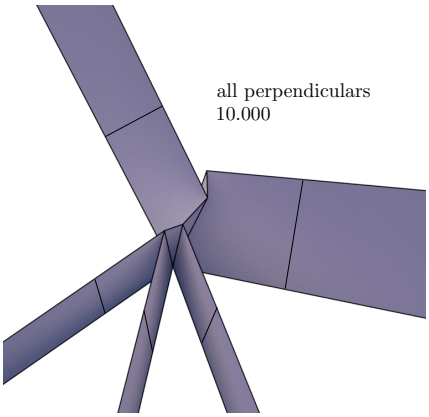

(c) Perpendicular structure, evolved mesh

Figure 10: An original mesh vertex is moved to satisfy the alternate angle condition (a). The perpendicular structures of the original mesh and the evolved mesh are shown in (b) and (c).

we guarantee that a solution to the linear system (3) corresponds to a *positive* set of offset rates? Based on our explorations, we conjecture that the answer may be 'always' or 'almost always', at least in the cases of primary interest in an architectural setting. A second task is to determine the best methods for optimizing an original mesh toward a similar mesh that is an FEO mesh.

A common theme throughout research on offsets is the requirement of design trade-offs. Whether it is a restriction of the input geometry (Pottmann and Wallner 2008; Pottmann et al. 2007; Wang and Liu 2010), increased support structures to cover undesirable node collisions (Sevtsuk and Kalvo 2015) or the emergence of facelets as in the present work, all methods have their limitations. In turn this highlights the fact that the characterization of the space of 'constructible' doubly curved discrete surfaces is still an open problem. The offsetting techniques in the current paper provide the designer with the unmodified implications of their surface with respect to material thickness, support structure, and node resolution. From this data, it is then possible to proceed with project specific processing, such as input surface optimization, complex node design, or other techniques, thereby adding to the scope of the design freedoms available to the architectural design team.

Acknowledgements

We thank Chris Cappadoccia, Patrick Ingram, Al Fisher and Panagiotis Papanastasis for fruitful discussions on the content of this paper. We thank the anonymous reviewers for their comments and suggestions.

References

Aish, Robert, Erik Verboon, and Gustav Fagerström. 2014. "Topo-facade: envelope design and fabrication planning using topological mesh representations." In *FABRICATE 2014 Publication: Negotiating Design & Making,* edited by Fabio Gramazio, Matthias Kohler, and Silke Langenberg. GTA Verlag.

Diestel, Reinhard. 2010. *Graph theory.* 4th ed. Berlin: Springer-Verlag.

Grossman, Jerrold W., Devadatta M. Kulkarni, and Irwin E. Schochetman. 1994. "Algebraic graph theory without orientation." *Linear Algebra and its Applications* 212:289–307.

Pottmann, Helmut, Yang Liu, Johannes Wallner, Alexander Bobenko, and Wenping Wang. 2007. "Geometry of Multi-layer Freeform Structures for Architecture." *ACM Trans. Graph.* 26 (3).

Pottmann, Helmut, and Johannes Wallner. 2008. "The focal geometry of circular and conical meshes." *Advances in Computational Mathematics* 29 (3): 249–268.

Ross, Elissa, and Daniel Hambleton. 2015. "Exact face-offsetting for polygonal meshes." In *Computational Ecologies: Design in the Anthropocene Proceedings of the 35th Annual Conference of the Association for Computer Aided Design in Architecture,* edited by Lonn Combs and Chris Perry, 203–209. ACADIA.

Sevtsuk, Andres, and Raul Kalvo. 2015. "Geometrical Solution Space for Grid Structures with Double-Walled Edges." In *Advances in Architectural Geometry 2014,* edited by Philippe Block, Jan Knippers, J. Niloy Mitra, and Wenping Wang, 215–231. Springer International Publishing.

Strang, Gilbert. 2009. *Introduction to Linear Algebra.* 4th ed. Wellesley: Wellesley-Cambridge Press.

Wang, Wenping, and Yang Liu. 2010. "A note on planar hexagonal meshes." In *Nonlinear Computational Geometry,* 221–233. New York: Springer.

Wang, Wenping, Johannes Wallner, and Yang Liu. 2007. "An angle criterion for conical mesh vertices." *Journal for Geometry and Graphics* 11 (2): 199–208.

West, Douglas B. 2001. *Introduction to Graph Theory.* 2nd ed. Upper Saddle River: Prentice Hall.